AMERICAN SOCIETY FOR MICROBIOLOGY | mBio®

RESEARCH ARTICLE

Transcriptional Mechanisms of Thermal Acclimation in *Prochlorococcus*

Laura Alonso-Sáez,[a] Antonio S. Palacio,[a] Ana M. Cabello,[a*] Semidán Robaina-Estévez,[b] José M. González,[b] Laurence Garczarek,[c] Ángel López-Urrutia[d]

[a]AZTI, Marine Research, Basque Research and Technology Alliance (BRTA), Sukarrieta, Spain
[b]Department of Microbiology, University of La Laguna, La Laguna, Spain
[c]Sorbonne Université, CNRS, UMR 7144 Adaptation and Diversity in the Marine Environment (AD2M), Station Biologique de Roscoff (SBR), Roscoff, France
[d]Centro Oceanográfico de Gijón, Instituto Español de Oceanografía, IEO-CSIC, Gijón, Asturias, Spain

ABSTRACT Low temperature limits the growth and the distribution of the key oceanic primary producer *Prochlorococcus,* which does not proliferate above a latitude of ca. 40°. Yet, the molecular basis of thermal acclimation in this cyanobacterium remains unexplored. We analyzed the transcriptional response of the *Prochlorococcus marinus* strain MIT9301 in long-term acclimations and in natural *Prochlorococcus* populations along a temperature range enabling its growth (17 to 30°C). MIT9301 upregulated mechanisms of the global stress response at the temperature minimum (17°C) but maintained the expression levels of genes involved in essential metabolic pathways (e.g., ATP synthesis and carbon fixation) along the whole thermal niche. Notably, the declining growth of MIT9301 from the optimum to the minimum temperature was coincident with a transcriptional suppression of the photosynthetic apparatus and a dampening of its circadian expression patterns, indicating a loss in their regulatory capacity under cold conditions. Under warm conditions, the cellular transcript inventory of MIT9301 was strongly streamlined, which may also induce regulatory imbalances due to stochasticity in gene expression. The daytime transcriptional suppression of photosynthetic genes at low temperature was also observed in metatranscriptomic reads mapping to MIT9301 across the global ocean, implying that this molecular mechanism may be associated with the restricted distribution of *Prochlorococcus* to temperate zones.

IMPORTANCE *Prochlorococcus* is a major marine primary producer with a global impact on atmospheric CO_2 fixation. This cyanobacterium is widely distributed across the temperate ocean, but virtually absent at latitudes above 40° for yet unknown reasons. Temperature has been suggested as a major limiting factor, but the exact mechanisms behind *Prochlorococcus* thermal growth restriction remain unexplored. This study brings us closer to understanding how *Prochlorococcus* functions under challenging temperature conditions, by focusing on its transcriptional response after long-term acclimation from its optimum to its thermal thresholds. Our results show that the drop in *Prochlorococcus* growth rate under cold conditions was paralleled by a transcriptional suppression of the photosynthetic machinery during daytime and a loss in the organism's regulatory capacity to maintain circadian expression patterns. Notably, warm temperature induced a marked shrinkage of the organism's cellular transcript inventory, which may also induce regulatory imbalances in the future functioning of this cyanobacterium.

KEYWORDS marine, *Prochlorococcus*, thermal acclimation, transcriptomics, cyanobacteria

Prochlorococcus is the most abundant photosynthetic organism on Earth (1) and a major contributor to oceanic primary production (2). Despite sustaining vast populations at the global scale, *Prochlorococcus* exhibits an enigmatic distribution in the ocean, with a sharp latitudinal barrier at ca. 45°N and 40°S (3, 4). While the ultimate reasons for such restricted

Editor Jennifer B. H. Martiny, University of California, Irvine

Address correspondence to Laura Alonso-Sáez, lalonso@azti.es.

*Present address: Ana M. Cabello, Centro Oceanográfico de Málaga, Instituto Español de Oceanografía, IEO-CSIC, Fuengirola, Málaga, Spain.

This paper is contribution 1152 from AZTI (Marine Research Division).

The authors declare no conflict of interest.

Received 7 December 2022
Accepted 21 March 2023
Published 13 April 2023

distribution are still unknown and may involve biotic interactions (5), temperatures in the range of 12 to 15°C typically limit the growth of *Prochlorococcus* in culture (3, 6, 7) and *in situ* (3), potentially representing critical thresholds for the metabolism of this cyanobacterium. Due to genome streamlining, *Prochlorococcus* is assumed to have a lower regulatory capacity than other phytoplankton groups and a limited metabolic flexibility to adapt to environmental disturbance, including temperature changes (8–10). However, a mechanistic understanding of *Prochlorococcus*' temperature sensitivity at the molecular level is still lacking.

In general, addressing the impact of temperature on the functioning of any organism is complex, as this parameter has overriding effects on virtually every aspect of cell physiology. Temperature notably impacts the cellular size, stability, and conformation of macromolecules and the kinetics of biochemical reactions, altogether leading to differences in cell growth (11). In the case of photosynthetic organisms such as *Prochlorococcus*, growth is closely linked to the photosynthetic capacity, which is also impacted by temperature (12–14). Under temperature conditions below the optimum, the slowdown in carbon fixation rates constrains the replenishment of terminal acceptors of the photosynthetic electron flow, producing an imbalance between photochemistry and metabolism. Under these conditions, the excess of light energy absorbed can generate cell-damaging reactive oxygen species (ROS), which need to be counterbalanced by photoprotective mechanisms (15). Under heat stress conditions (35 to 50°C), ROS are also typically produced, likely not as a result of an excess of energy absorbed, but as a result of heat-induced structural and functional changes in the photosystems and thylakoid membranes (16). The decline in photosynthetic activity in phototrophs under moderate warm stress has been associated with different processes, including the inhibition of *de novo* synthesis of the photosystem II D1 protein by ROS (17), the inactivation of the oxygen-evolving complex (18), and declines in electron transport (19).

At the expression level, a variety of compensatory mechanisms have been found to be activated in several phytoplankton groups (i.e., *Synechococcus* and eukaryotic phytoplankton) to preserve cell functioning under thermal stress conditions (12–14, 20–23). The cold stress response network involves the upregulation of fatty acid desaturases to offset decreases in membrane fluidity at low temperature and RNA helicases and cellular chaperones to facilitate proper folding of nucleic acids and proteins (21, 22, 24, 25). Low temperature can also impact the expression of central components of the transcriptional and translational machinery in eukaryotic phytoplankton, which are upregulated to compensate for their reduced efficiency (21, 26), and even impact global regulatory networks, such as circadian rhythms in cyanobacteria (27). At elevated temperatures, a nearly universal response induces the expression of heat shock proteins, which degrade or restructure denatured proteins and nucleic acids (28).

Some of the temperature compensatory mechanisms involve only short-term transcriptional responses until cell functioning is restored (25). In other cases, the baseline expression of key enzymes is upregulated under long-term cold acclimations (26). Beyond short-term temperature manipulation experiments, where cells are suddenly exposed to a "thermal shock," understanding mechanisms of long-term acclimation is particularly relevant as they more accurately reflect responses to gradually changing thermal conditions. Here, we performed a series of experiments on *Prochlorococcus marinus* MIT9301, where cells were progressively exposed from a temperature close to their optimum to their upper and lower thresholds of growth. This strain, which is a representative of the *Prochlorococcus* dominant clade *in situ* (HLII) (29, 30), was selected because it shares the highest sequence similarity with environmental sequences (31) and enabled the identification of closely related transcripts in natural *Prochlorococcus* populations. We first used a quantitative transcriptome sequencing (RNA-Seq) approach (32, 33) to decipher the transcriptional response of MIT9301 to temperature acclimations. Then, we addressed the environmental relevance of one of the most conspicuous transcriptional responses observed in MIT9301, involving highly expressed photosynthetic genes, in oceanic metatranscriptomes collected along a comparable thermal gradient. Our objective

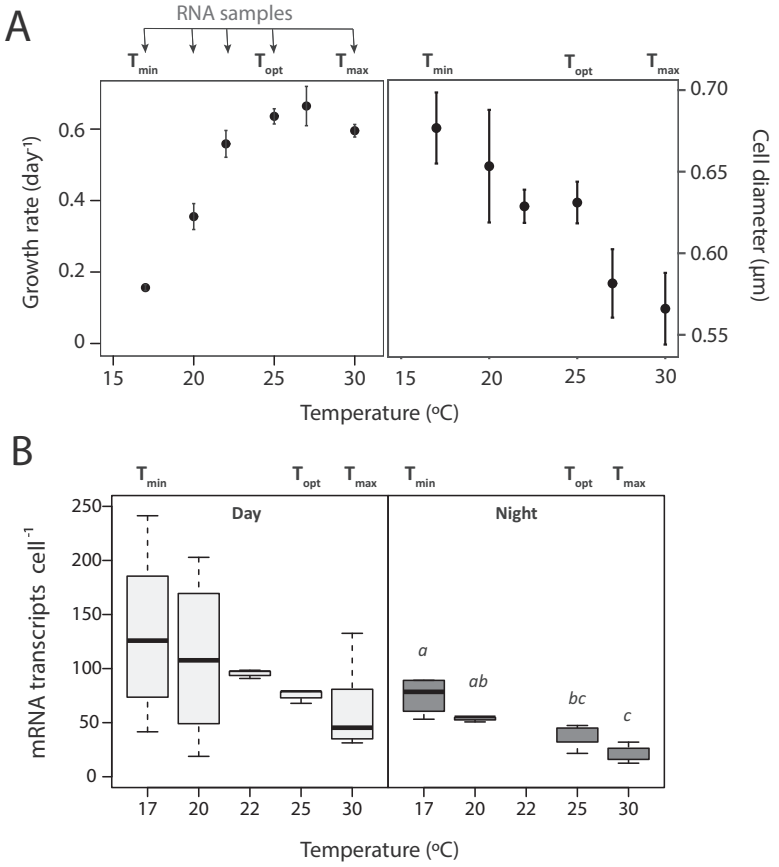

FIG 1 Growth rates, cell size, and number of mRNA transcripts per cell in samples of *Prochlorococcus marinus* MIT9301 collected after long-term thermal acclimation. Between 3 and 7 biological replicate samples are represented, depending on the temperature treatment, and error bars report the standard deviation between replicates. On the top of each plot, the minimum (T_{min}), optimum (T_{opt}), and maximum (T_{max}) temperatures are indicated, and additionally, in the upper left plot, temperature treatments where RNA samples were collected are shown with arrows. (A) Growth rate and size of MIT9301 cells along the thermal niche. (B) Estimates of mRNA transcripts per cell along the thermal niche in samples collected at daytime (left panel) and nighttime (right panel). Lowercase italic letters denote statistically significant differences (analysis of variance [ANOVA] and Tukey *post hoc* test; $P < 0.001$).

was to analyze how sustained growth at suboptimal temperature reprograms the transcriptome of *Prochlorococcus* and significantly advance our understanding of which mechanisms underlie the organism's growth restriction under cold and warm conditions.

RESULTS

Thermal acclimation experiments with *Prochlorococcus marinus* MIT9301: growth rates and mRNA content. MIT9301 cultures were synchronized to a diel 12-h/12-h light/dark cycle and long-term acclimated to six temperatures along the organism's thermal range (Fig. 1; see Fig. S1 in the supplemental material). MIT9301 could not survive single-generation transfers below 17°C or above 30°C, and thus, these were considered minimum and maximum temperature thermal thresholds for this strain (here, T_{min} and T_{max}, respectively). The growth rate of MIT9301 increased from 0.17 day^{-1} at T_{min} to ca. 0.61 day^{-1} at 25°C (here referred to as the optimum growth temperature [T_{opt}]) and thereafter entered a warm stress zone up to 30°C, where no further increases in growth rate were observed (Fig. 1A). The average size of MIT9301 cells also changed along the thermal gradient, with maximum and minimum values at the T_{min} and T_{max}, respectively (Fig. 1A).

After the acclimation period, RNA samples were collected under five different temperature conditions 3 h after subjective sunrise and sunset (daytime and nighttime, respectively) (see Table S1 in the supplemental material). Large variations in the number of mRNA transcripts per cell were found in replicate cultures acclimated to 17 and 20°C during daytime,

while values were highly constrained in temperatures close to the optimum (22 and 25°C) (Fig. 1B). A pattern of decrease of mRNA transcripts with increasing temperature was found, with the average number of mRNA transcripts per cell being positively correlated with cellular size in nighttime samples (Spearman $\rho = 0.89$; $P < 0.001$).

Quantitative global transcriptomic analysis of MIT9301 in experimental long-term acclimations. The top-expressed genes in MIT9301 were associated with photosynthetic components (e.g., *psbA* and *psbC*), the RuBisCO enzyme (*rbcL*) or an ammonium transporter (*amt*), which reached average values above two mRNA transcripts per cell (Table S2 and Table S3). However, the average abundance of most mRNA transcripts was at least 1 order of magnitude below that value, which indicates that only a fraction of the population was actively expressing them at any given time. Estimates of mRNA transcript abundance were normalized by cell biovolume (i.e., transcripts per cubic micrometer, or [mRNA]) (Table S4), to discard potential indirect effects of cell size on transcript abundance in further analyses.

A substantial fraction of MIT9301 genes were differentially expressed along the temperature gradient (i.e., exhibited significant variations in cellular [mRNA] estimates at different temperatures). In total, 61% of MIT9301 protein-coding genes were differentially expressed at nighttime, while this number was reduced to 30% during daytime (Kruskal-Wallis test; $P < 0.05$), in association with an increase in the variability of gene expression levels; while [mRNA] values of individual genes in different biological replicates were highly constrained at the T_{opt}, a large variation was found during daytime at both thresholds of growth and particularly at the T_{min} (Fig. 2 and 3; Table S4). This suggests a reduced ability of MIT9301 cells to maintain a tight transcriptional control under challenging temperature conditions when cells are exposed to light. Notably, the expression of some sigma factors and key regulatory proteins from different families also showed this pattern (Fig. 3A and B).

We identified five clusters of genes according to their patterns of daytime and nighttime expression at different temperatures (Fig. 2). More than 90% of MIT9301 protein-coding genes were assigned to one of these clusters with a probability score of >0.5 (Table S5), which indicates that these clusters were highly representative of the main thermal gene expression responses in this strain. Clusters A and E were represented by genes involved in core cellular and metabolic processes typically expressed in *Prochlorococcus* during daytime and nighttime, respectively (34). Clusters C and D were associated with mechanisms of cold stress response, as they were characterized by a strong upregulation at the T_{min} either during daytime or during both daytime and nighttime, respectively. Finally, the expression of genes in cluster B showed a decreasing trend from the T_{opt} toward the T_{min} during daytime (Fig. 2), paralleling the pattern observed in growth rates along the thermal niche (Fig. 1A). Therefore, we hypothesize that the expression of cluster B genes is associated with metabolic processes limiting the growth of *Prochlorococcus* when exposed to cold conditions.

Cluster A included genes related to C fixation and assimilation, such as RuBisCO (*rbcLS*), CO_2 transporters (*csoS2*), carboxysome shell proteins (*ccmK*), the Calvin cycle (e.g., *gap2*, *tktA*, *glpX*, *pgk*, and *cbbA*), and glycogen synthesis (*glgABC*), consistently expressed during daytime along the thermal gradient (Fig. 2; Table S4 and Table S5). This cluster also included ATP synthesis genes (*atpADE*) and a few components of photosystem II (PS II) (*psbA*, *psbC*, and *psbD*). Cluster E included genes related to catabolic consumption (*cyoB* and *ndhD*), DNA replication (*dnaA*, *nrdJ*, and *gyrB*), cell division (*ftsZYQ*), and the pentose phosphate pathway (*tal*, *gnd*, and *zwf*), all of them upregulated at nighttime. Altogether, these essential pathways likely represent a transcriptional core, which *Prochlorococcus marinus* MIT9301 maintains under all temperature conditions.

Clusters C and D genes included different elements of the global stress response, such as cellular chaperones (*groES/groES*, *dnaK*, and *clpBCP*) (35, 36) and fatty acid desaturases (*desA* and *desC*), as well as mechanisms against oxidative damage, such as DNA repair (*recA* and *ruvB*) (37, 38), superoxide dismutase (*sod*), and the synthesis of antioxidant compounds like carotenoids (*pds* and *crtBH*) and rubredoxin (*rub*) (Fig. 2 and 3; Table S5). Notably, the expression of the chaperones *groEL/groES*, *grpE*, and *htpG* was strongly upregulated at the T_{min} only during daytime, suggesting a prioritization of their expression during the light-exposed period (Fig. 3C). Other metabolic processes upregulated at the T_{min} were the mobilization

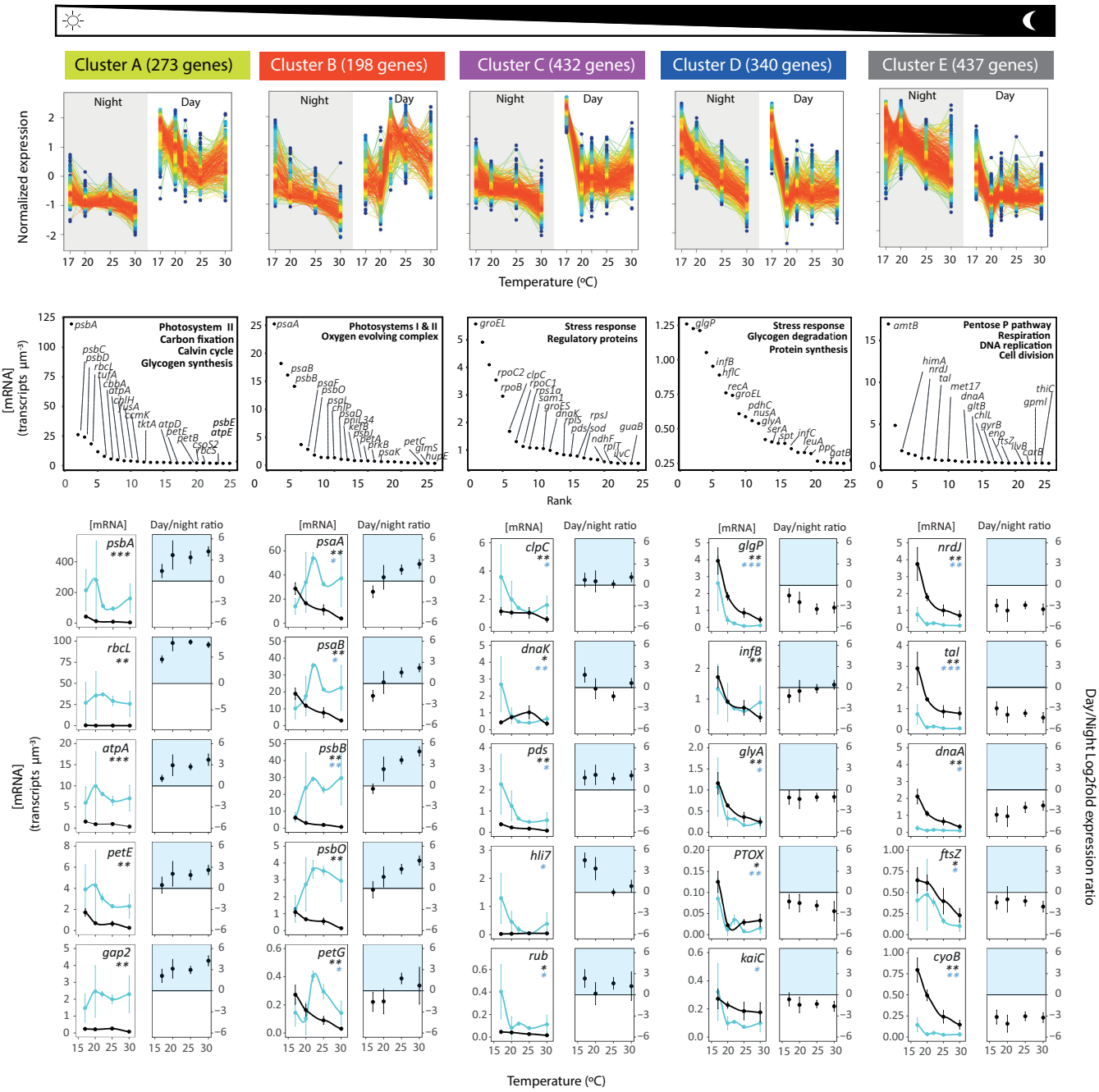

FIG 2 Clusters of *Prochlorococcus marinus* MIT9301 genes according to their pattern of daytime and nighttime expression along the thermal niche. Within each cluster, the right and left panels represent daytime and nighttime expression of the same genes, respectively. Dot colors indicate local density at each point of the scatterplot, with red circles indicating a high density of dots. Line colors within each SoftCluster indicate the membership value assigned by the fuzzy c-means soft clustering of each gene, ranging from 1 (red, high score) to 0.5 (blue, low score). Genes with a membership value lower than 0.5 are not plotted, and neither are they included in the total number of genes for each cluster (but they are included in Table S5). Below each cluster, the top 20 genes expressed are shown in rank order plots, and the expression levels (measured as [mRNA] and day/night $\log_2$ fold expression ratio) of a selection of representative genes are shown. Daytime values appear as blue lines and nighttime values as black lines. Between 3 and 7 biological replicate samples are represented, depending on the temperature treatment and error bars report the standard deviation between replicates. Asterisks in the plots denote significant differences in transcript concentration along the thermal gradient in daytime (blue asterisks) or nighttime (black asterisks) according to the Kruskal-Wallis test (*, $P < 0.05$; **, $P < 0.01$; ***, $P < 0.001$). In the $\log_2$ fold ratios, values above 0 represent preferential expression during daytime (highlighted in blue), while values below 0 represent preferential expression during nighttime.

of energy storage (i.e., glycogen degradation, *glgP*), and the synthesis of proteins, as reflected by the increase in the [mRNA] of amino acid synthesis genes (*glyA*, *serA*, and *leuA*), translation initiation factors (*infABC*) and N acquisition genes (Fig. 2 and 3; Table S4).

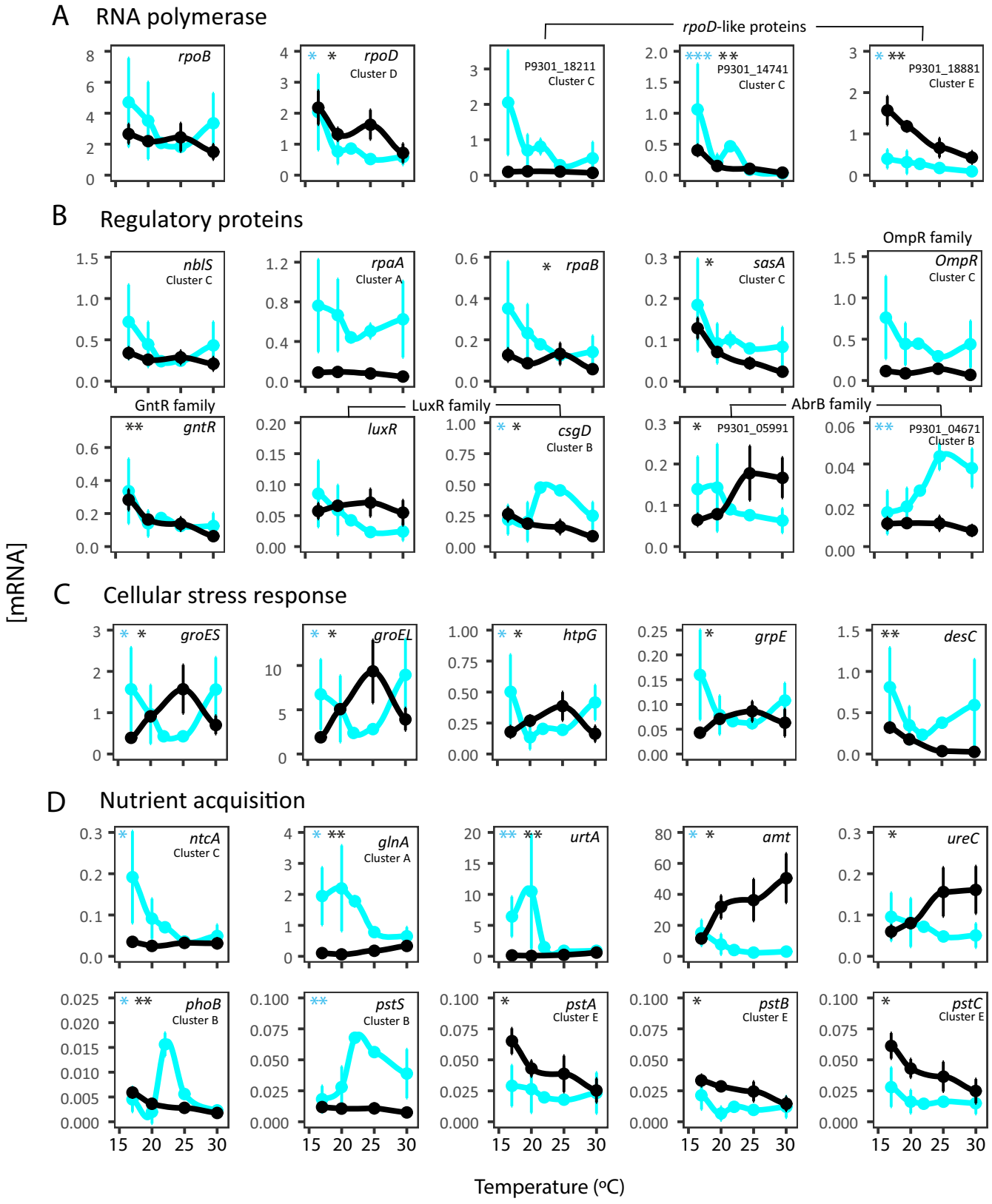

FIG 3 Cellular expression levels (measured as [mRNA]) in *Prochlorococcus marinus* MIT9301 during daytime (blue lines) and nighttime (black lines) along the thermal niche of (A) RNA polymerase components, including sigma factors, (B) histidine kinases and other regulatory proteins, (C) genes involved in the stress response, and (D) nitrogen and phosphate acquisition genes. Asterisks denote significant differences in transcript concentration along the thermal gradient in daytime (blue asterisks) or nighttime (black asterisks) according to the Kruskal-Wallis test (*, $P < 0.05$; **, $P < 0.01$; ***, $P < 0.001$). The SoftCluster membership of each gene is shown only for those cases where the probability score was >0.80.

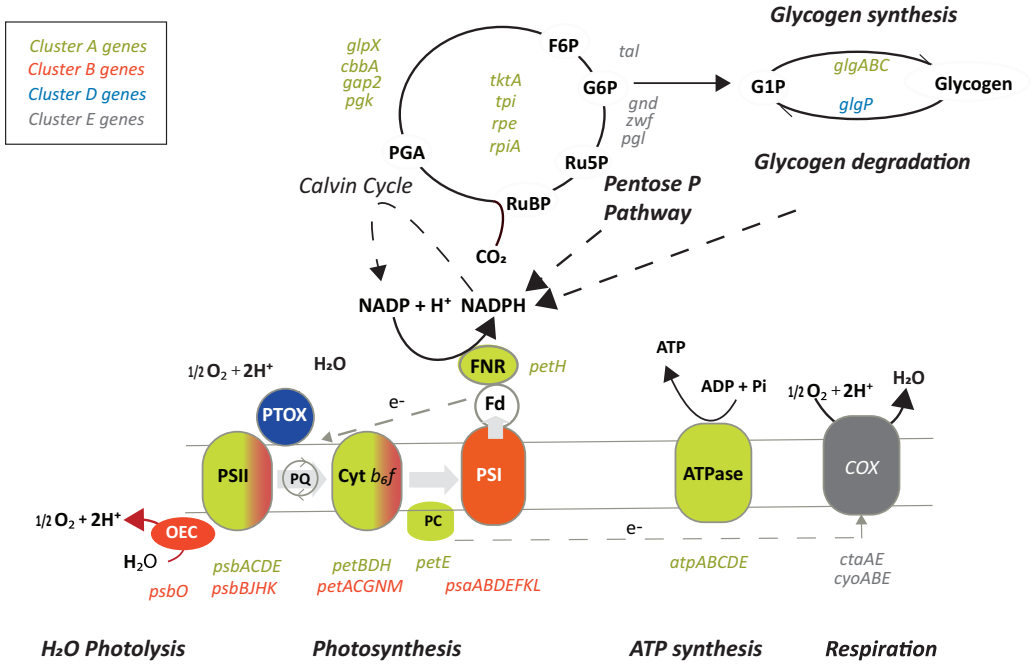

FIG 4 Schematic diagram showing some of the main components of the photosynthetic and carbon metabolism pathways in *Prochlorococcus*. Colors of genes (or their corresponding protein complexes) follow the same code as their respective SoftClusters in Fig. 2.

The strong upregulation of N acquisition mechanisms at the T_{min} under light conditions was observed not only for genes predominately expressed during daytime at the T_{opt} (i.e., the global nitrogen regulatory protein gene *ntcA*, *glnA*, and urea transporter genes), but also for genes typically expressed at nighttime in *Prochlorococcus*, such as the ammonium transporter (*amt*) and urease (*ureABC*) genes (Fig. 3D; Table S4). This likely reflects the large cellular demand of N for protein synthesis during daytime under cold stress conditions. In the case of phosphate uptake, the high-affinity ABC transporter *pstABC* genes were upregulated under cold conditions at night, following the pattern of cluster E genes, possibly related to the cellular demand of P for DNA replication. In contrast, both copies of the periplasmic phosphate binding protein (*pstS*) showed maximum expression values around the T_{opt} during daytime, following the pattern of most photosynthetic genes (cluster B), which highlights the complexity of the thermal response of nutrient acquisition genes (Fig. 3D).

Finally, the expression of all components of the PS I complex (*psaABDEFKL*) and some of PS II (including *psbBJH* and the oxygen-evolving complex protein *psb*O) showed a gradual decrease in expression from a temperature close to the optimum to the $T_{min,}$ (Fig. 2) in correlation with MIT9301 growth rates (Fig. 1). This expression pattern was different from those of other PSII components (*psbACD* [described above]), which were not differentially expressed during daytime along the thermal niche (Kruskall-Wallis; $P > 0.05$) (Fig. 2). Similarly, many components of the photosynthetic electron transport genes were assigned to either cluster B (*petACGNM*) or cluster A (*petBEDH*), implying a nonuniform transcriptional thermal response of all components of the photosynthetic apparatus (Fig. 4). Yet, a general pattern of upregulation of photosynthetic genes during nighttime under cold conditions was observed (Fig. 2), inducing changes in their day/night $\log_2$ fold expression ratio. This result suggests a loss in the capacity of cells to regulate their circadian expression under cold conditions. Accordingly, the day-night expression patterns of the circadian clock *kaiBC* genes were also impaired at the T_{min} (Fig. 2).

Transcriptional response of photosynthetic genes in naturally occurring *Prochlorococcus* populations. After addressing the impact of thermal acclimation on MIT9301, we next aimed to test whether the transcriptional suppression of photosynthetic

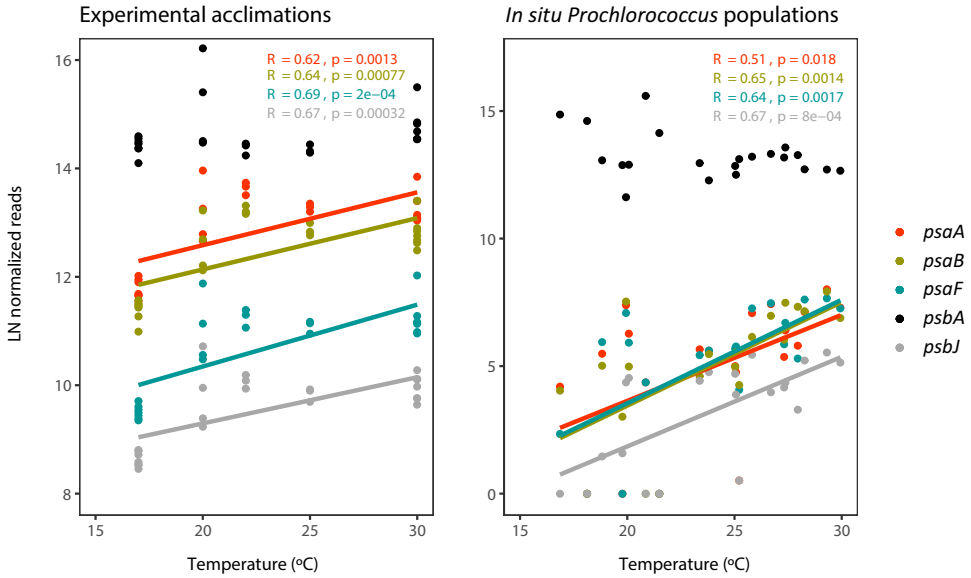

FIG 5 Expression patterns of a selection of *Prochlorococcus* photosynthetic genes of photosystem II (*psbA* and *psbJ*) and photosystem I (*psaA*, *psaB*, and *psaF*) along the thermal gradient 17 to 30°C in experimental acclimations (as analyzed in *P. marinus* MIT9301 by transcriptomics [left panel]) and *in situ* environmental conditions (as analyzed in reads mapping to MIT9301 identified in metatranscriptomes of the *Tara* Oceans data set [right panel]). In both cases, reads were normalized using DESeq2 and log transformed. Linear regression lines are shown for all genes with significant Spearman correlation coefficients at a *P* value of <0.05 (indicated in the plots).

genes at the cold temperature observed experimentally was also found in natural *Prochlorococcus* populations *in situ*. For this, we identified reads closely related to MIT9301 in the *Tara* Oceans metatranscriptome data set (39), including samples distributed across different ocean basins along a comparable thermal gradient (Table S6). The number of reads mapping to MIT9301 (≥98% identity following our two-step filtering strategy [see Materials and Methods]) ranged from 6,379 to 9.62 million in the different environmental samples (Table S7). The DESeq2-normalized abundance of transcript counts from some of the most actively expressed genes of PS II (*psbA* and *psbD*) did not show any significant trend along the *in situ* thermal gradient from 17 to 30°C (Spearman correlation; $P > 0.05$), mirroring the response observed under culture conditions (Fig. 5; Fig. S2). In contrast, other PS II components (*psbJ*) were positively correlated with temperature in both the experimental and *in situ* data sets (Spearman $R = 0.6$; $P < 0.01$), indicating a downregulation at cold temperature (Fig. 5). Similarly, the downregulation of PS I genes at cold temperature was clearly observed both in the experimental and *in situ* data sets (Fig. 5), reinforcing the environmental relevance of this response. Temperature had the strongest correlation to photosynthetic transcript counts in comparison with all other tested environmental variables (Fig. S3), indicating that these correlations were not driven by covarying environmental parameters.

DISCUSSION

There is a remarkable gap of fundamental knowledge of the molecular mechanisms of thermal acclimation in *Prochlorococcus*, as previous studies have concentrated on their cyanobacterial sister clade *Synechococcus* and eukaryotic phytoplankton (12–14, 20–22, 40, 41). Acquiring this knowledge is crucial for answering a long-standing question: what limits the ability of *Prochlorococcus* to expand to high-latitude environments? The decrease in the light-harvesting capacity of phytoplankton under cold conditions has been typically attributed to changes in the conformation of membrane lipids and proteins of their photosynthetic apparatus (14, 42). Our quantitative gene expression analysis shows that, in the case of *Prochlorococcus*, the inability to maintain the organism's photosynthetic capacity under cold conditions is already critically compromised at the transcriptional level, as we found a clear suppression of the expression of most photosynthetic genes under cold conditions. The same pattern was found for reads mapping to MIT9301 in *in situ* metatranscriptomes

across the global ocean, suggesting that this molecular mechanism may be relevant to explain the restricted distribution of *Prochlorococcus* to temperate zones. Notably, this response differs from those of previous studies targeting diatom cultures (26) or phytoplankton communities *in situ* (21, 39), indicating fundamental differences in the ability of *Prochlorococcus* to respond to cold temperature, which may be related to the organism's exceptionally high sensitivity to oxidative stress (38, 43, 44).

Photosystems are naturally sensitive to light damage, which is exacerbated under low temperature (22). The cellular decision to shut down the sunlight energy conversion system under cold conditions likely arises from the inability of *Prochlorococcus* to cope with uncontrolled redox chemistry when there is an imbalance between the production of excited electrons by light and their metabolic consumption. The downregulation of photosystems would represent an emergency mechanism to slow down the electron flow and prevent the production of cell-damaging ROS (45, 46). Notably, the response was not equal for all photosystem components, as previously observed in cultured *Prochlorococcus* strains undergoing other types of stress, such as iron starvation (47), phage infection (48), or high light exposure (49). On the one hand, the high expression of *psbA* transcripts under all temperature conditions is likely related to the need to maintain an exceptionally high turnover rate of this protein (50), being under a different regulatory regime from other PS components (34, 51, 52). On the other hand, the selective downregulation of PS I probably arises from the strong need to protect PS I from oxidative stress, as this photosystem typically lacks efficient repair machinery, and therefore its damage may be practically irreversible (53). Interestingly, MIT9301 also upregulated the plastoquinol terminal oxidase (PTOX) at the T_{min} (Fig. 2), which is thought to function as a safety valve in cyanobacteria to avoid electron flow toward PS I (54).

In addition to the transcriptional suppression of photosynthetic genes, we found that under light conditions, cold temperature induced a loss in the regulatory capacity of MIT9301 cells (Fig. 2). This was reflected in the loss of the circadian day/night gene expression ratio and the increased variability in the concentration of cellular mRNA transcripts among biological replicates. In a previous study, it was suggested that higher levels of stochasticity in *Prochlorococcus* gene expression during the transition from photosynthesis to the use of internal energy is related to the accumulation of ROS (55). Our transcriptomic results are consistent with the idea of oxidative stress impacting the regulatory capacity of *Prochlorococcus*, as we found the upregulation of different genes against this source of stress under cold conditions (Fig. 2 and 3). Notably, at the T_{min} we observed a high variability in the expression of regulatory proteins that modulate the cellular response to daily light fluctuations in cyanobacteria, including sigma factors (*rpoD*) (56, 57), the NblS-RpaB two-component system (58), and the SasA-RpaA clock output system (59, 60) (Fig. 3). Assuming that mRNA transcript levels reflect the protein levels of these regulators, our results would imply a critical impairment of their coregulated networks. Other mechanisms of transcriptional regulation in *Prochlorococcus* (i.e., RNA-based regulatory strategies) (61) were likely also compromised at low temperature, as evidenced by the upregulation of the RNase *rne* gene at the T_{min} (see Table S4 in the supplemental material).

Marked changes in the day/night gene expression ratio of some of *Prochlorococcus* key functional genes along the thermal niche imply a deregulation of one of their fundamental features: i.e., the coordination of transcriptional oscillations with the daily light/dark cycle. This feature is key to optimize cellular processes through anticipating and synchronizing transcription of photosynthetic genes with daylight hours (34, 62, 63). At T_{opt}, the day/night expression preferenda of most key functional genes of MIT9301 matched those previously observed in the model strain MED4 (34), reinforcing the idea that maintaining this transcriptional choreography is a highly conserved and critical trait. The deregulation observed at the cold temperature led to the paradoxical situation where, after subjective sunrise, chilled *Prochlorococcus* MIT9301 cells contained severalfold less PS I transcripts than after subjective sunset, which supports the idea of a malfunctioning regulatory network (Fig. 2). With only two samplings over the daily cycle, we cannot ensure whether the observed changes were due to random misregulations or variations in the phasing or

amplitude of their diel gene expression patterns. Yet, considering that we were sampling the two daily periods when most *Prochlorococcus* genes show maxima in expression (34), the inversion of their day/night preferenda is remarkable and likely has an important impact on *Prochlorococcus* fitness.

In contrast to the pattern observed in day-time samples, genes related to *Prochlorococcus* cell division cycle, typically expressed during nighttime, showed rather constrained [mRNA] values between replicates. We observed an increase in [mRNA] of those genes toward cold conditions, which may be related to the predominant cell cycle phase of the cells. As the timing of cell division is delayed in *Prochlorococcus marinus* MIT9301 when acclimated to cold temperature (64), our results likely reflect a situation where a higher proportion of cells were still undergoing the S phase at 17°C and 20°C at the time of sampling (i.e., 3 h after subjective dusk) compared to other acclimation temperatures.

At the warm temperature threshold, the upregulation of a variety of cellular chaperones (e.g., *groEL/groES*, *htpG*, and *grpE*) reflected that cells were undergoing substantial stress. However, no drastic changes were generally observed in the expression of most protein-coding genes at the T_{max}. Accordingly, a previous study on the short-term response of MED4 to warm stress found that the synthesis of new polypeptides was not induced (65). We had previously shown that *Prochlorococcus* MIT9301 cells decrease in size after long-term warm acclimation, in accordance with the temperature-size rule (64). Interestingly, here, we found a conspicuous streamlining in the transcript inventory of cells in parallel with the progressive reduction in cell size (Fig. 1). While at nonrestricting growth temperature, the average estimate of mRNA transcript abundance per cell was within the range reported for environmental marine bacteria (i.e., ca. 85 to 255 transcripts per cell) (32), under warm conditions this average dropped down to 30 mRNA transcripts of protein-coding genes per cell at nighttime. At increasing temperatures, cells may require a lower mRNA content to achieve the same translation rates, as suggested for rRNA content in the translation-compensation hypothesis (66). Yet, it should be considered that cellular reactions involving small numbers of molecules are intrinsically noisy, being dominated by fluctuations in concentration and stochasticity (67, 68). Thus, the decline in the transcript inventory under warm conditions also invites the hypothesis that there is a critical threshold in the number of mRNA copies beyond which cells lose regulatory capacity, contributing to the growth arrest.

In summary, previous studies on phytoplankton have identified the cellular membrane and translational apparatus as central elements associated with the thermal adaptation at the transcriptional level (21, 26). Some of these mechanisms were also observed in MIT9301, such as the cold upregulation of the translational machinery, likely to compensate for the general slowdown in protein synthesis rates, and fatty acid desaturases critical for maintaining the fluidity of cellular membranes (24). Yet, we found that in the case of *Prochlorococcus*, a general downregulation of photosystem components and impairment in their circadian expression patterns emerged as major features potentially impacting their physiology when approaching cold conditions. Low temperature has been previously shown to nullify the circadian rhythm in different organisms, including plants and different phytoplankton species, moving the circadian oscillation to a damped oscillation (see references in reference 27). *Prochlorococcus* contains only a minimalist circadian system; thus, its cell cycle is likely more easily perturbed than that from organisms containing a complete *kaiABC* gene set. As oxidative stress relates to both the need to protect the photosynthetic machinery and the ability of *Prochlorococcus* species to "reset" their daily cycles in the morning hours (69), it is plausible to link this source of stress to the molecular response observed, but experimental evidence would be required to confirm this point.

The disruption of the transcriptional choreography in *Prochlorococcus* may be a differentiating factor compared to *Synechococcus* and eukaryotic phytoplankton, which do not require maintenance of such a fine-tuned daily expression rhythm to maintain their metabolism. The higher tolerance of *Synechococcus* species to oxidative stress (38) may also imply a more resilient photochemistry when exposed to cold conditions, enabling them to colonize higher latitudes. Additionally, we postulate that increased levels of stochasticity in gene expression under challenging temperature conditions may contribute to a decrease

in *Prochlorococcus* fitness. These remain as interesting hypotheses to test in future studies, with implications for the functioning of this global primary producer and, thus, marine carbon biogeochemistry under future oceanic conditions.

MATERIALS AND METHODS

Growth of cultures and temperature acclimation. We grew nonaxenic cultures of *Prochlorococcus marinus* MIT9301 obtained from the Roscoff Culture Collection (RCC) in PCR-S11 culture medium (70), based on Red Sea salt (Houston, TX, USA). Cultures were grown under a 12-h/12-h photoperiod and irradiance of 120 μmol quanta m^{-2} s^{-1} in polycarbonate flasks with vented caps. During the acclimation, we maintained the cultures in exponential growth by performing serial transfers before cell density reached 30% of the maximum yield. The acclimation started from 22°C (i.e., temperature of maintenance in RCC), and temperature was progressively changed toward the upper and lower thermal thresholds. At each acclimation step, the temperature was changed by a maximum of 2°C and down to 0.2°C when approaching the temperature thresholds, to avoid lethal thermal stress (see Fig. S1 in the supplemental material). We considered that the culture had been fully acclimated to a temperature treatment when the growth rate stayed stable in at least two consecutive growth curves after at least 8 generations. Flow cytometry was used for sustained monitoring of the culture growth during the acclimation process. Samples were fixed with glutaraldehyde (final concentration of 0.025%) for 10 min at room temperature and under dark conditions and frozen at −80°C until analysis in a FACSCalibur flow cytometer (Becton Dickinson). Estimates of cell diameter were obtained based on the natural logarithmic-transformed side scatter (SSC) using the calibration provided in reference 71. Cell volumes were calculated from the resulting estimates of cell diameter, assuming a spherical cell shape.

RNA sample collection and extraction. Once the cultures reached full acclimation to the temperatures selected (17, 20, 22, 25, and 30°C), we reinoculated biological replicate batch cultures into fresh medium (160 mL) and collected samples for RNA-Seq analysis during exponential growth (with cell density values ranging between 6×10^7 and 17×10^7 cells mL^{-1}) (see Table S1 in the supplemental material). For each temperature and biological replicate (ranging from 3 to 7, depending on the experimental treatment) (Table S1), samples for RNA extraction were collected 3 h after the onset and offset of the photoperiod (daytime and nighttime, respectively). Exceptionally, for the acclimation temperature 22°C, only daytime RNA samples were available. Samples were filtered on 0.22-μm-pore-size polyethersulfone (PES) filters using a vacuum pump at a pressure of 5 lb/in^2. Immediately after filtration, filters were snap-frozen in liquid nitrogen and stored at −80°C. The time elapsed from the start of the filtration until freezing was always less than 2 min.

Quantitative benchmarked RNA extraction was performed following reference 33 using five RNA standards from *Saccharolobus solfataricus* (formerly *Sulfolobus solfataricus*) P2 (NCBI Taxon ID 273057) obtained by *in vitro* transcription of genomic templates of the isolate (standards 3, 6, 7, 13, and 14, as described in reference 33). The filters were spiked with the RNA standards individually (10 to 28 μL) at a concentration of ca. 20 pg μL^{-1} prior to the initiation of the RNA extraction. Subsequently, RNA samples were extracted with the mirVana kit (Ambion), and DNA was removed using the TURBO DNase (Ambion). Samples were depleted from rRNA using the Ribo-Zero rRNA removal kit (Bacteria; Illumina), and a quality check was performed using a Bioanalyzer (Agilent). mRNA samples were concentrated using the Zymo Clean & Concentrator kit, and cDNA libraries were constructed using the TruSeq stranded mRNA sample preparation kit (Illumina). cDNA libraries were sequenced as 75-bp paired-end reads on an Illumina HiSeq v4 platform (CNAG, Spain).

Quantitative gene expression analysis of *Prochlorococcus* MIT9301 under culture conditions. The sequence read quality check was performed with the FastQC tool (72), and Trimmomatic (73) was used to trim raw sequences (SLIDINGWINDOW:50:35 and MINLEN:50) and pair those passing quality thresholds. rRNA sequences were removed using SortMeRNA (74), and the remaining reads were mapped with Bowtie2 (75) (using the "–non-deterministic" parameter) against the *Prochlorococcus marinus* MIT9301 genome (NCBI Taxon ID 167546). The same procedure was done with the *S. solfataricus* genome to identify RNA internal standard reads. Read count tables were obtained using HTSeq (76) with the following parameters: "–stranded = reverse -a 10 -m intersection-nonempty." Quantitative estimates of individual transcript abundance (Ta) of MIT9301 protein-coding genes in each RNA sample were obtained following the calculations described in (77): Ta = (Ts × Sa)/Ss. Ta corresponds to the estimated number of transcripts of an individual MIT9301 protein-coding gene, Ts corresponds to the number of reads assigned to the corresponding MIT9301 protein-coding gene, Sa corresponds to the molecules of internal RNA standards spiked to the RNA sample, and Ss corresponds to the number of reads assigned to *S. solfataricus* internal standards. In this calculation, one of the standards (standard 14) was removed from the analysis because it was consistently recovered in higher proportion than other standards. Ta values were divided by total cell abundance or estimates of total cell biovolume collected in the corresponding RNA filter to obtain estimates of transcript abundance per cell and per volume (i.e., transcript concentration), respectively (Table S1 to Table S3). This normalization is relevant because cell size, which varies over the thermal gradient in this strain (Fig. 1A), can impact the number of cellular transcripts (78, 79).

Bioinformatic analysis of transcriptional patterns of *Prochlorococcus* photosynthetic genes in oceanic samples and culture conditions. For comparison of the expression patterns of *Prochlorococcus* photosynthetic genes along the same thermal gradient under environmental and culturing conditions, two data sets were produced using a common normalization method (DESeq2) (80). The experimental data set was obtained from the raw read counts obtained by HTSeq2 in the long-term thermal acclimation experiments, as explained above. To obtain the environmental database, a data set of *Tara* Oceans metatranscriptomes (39) was initially selected based on the latitude range where *Prochlorococcus* is found in the ocean (i.e., between 45°N and S), the thermal range of MIT9301 (17°C to 30°C), and the time of sample collection (between 6 a.m. and 12 p.m., when the expression of photosynthetic genes should be close to their

maximum). Fastq sequence files were quality filtered with fastp (81) using default parameters, and rRNA sequences were removed with RiboDetector (82) with the option "–ensure" selected. The remaining reads were filtered to remove reads not affiliated with *Prochlorococcus*, using a custom-made database with the complete genome sequences in the MarRef database, which included 16 *Prochlorococcus* and 17 *Synechococcus* genomes (83), and eukaryotic genes of interest extracted from Refseq (84): i.e., *psaA*, *psaB*, *psaD*, *psaF*, *psaL*, *psbA*, *psbD*, and *psbO*, searched with Entrez filter [Gene Name] AND ((protists[filter] OR plants[filter]) AND refseq[filter]). Metatranscriptome sequences closest to *Prochlorococcus* were identified based on blastn v.2.12.0+ searches (identity of ≥98% and bitscore of ≥30), and only those with the highest bitscore to *Prochlorococcus* sequences were considered further. Subsequently, we applied a two-step filtering strategy to obtain read counts closely related to MIT9301. First, we aligned each metatranscriptome sample against the MIT9301 genome using BWA mem v.0.7.17-r1188 with default parameters (85). Next, we discarded alignments that had a percentage of identity lower than 98%, a read length lower than 50 bases, and a number of matches lower than 50% of the total length of each aligned sequence. The percentage of identity was computed as $100 \times [N\_m/(N\_m + N\_i)]$, where N_m corresponds to the number of matches in the alignment and N_i to the number of mismatches. The number of matches was obtained by parsing the MD tag of the alignment record, while the number of matches and mismatches was obtained from the CIGAR string in the SAM file. Once alignments were filtered, we proceeded to count aligned reads with HTSeq v.2.0 with default parameters (86). Next, we removed noncoding genes from the count matrices as well as genes that had no counts across all conditions, to facilitate the consequent normalization. We also discarded samples that had counts of less than 10 genes other than the *psbA* gene. Finally, we normalized count data using the default DESeq2 v.3.15 count normalization workflow (80). All analyses were assisted with customized Python code (87) available at https://github.com/Robaina/prochlorococcus (88).

SoftClustering and statistical analyses. Clusters of differentially expressed genes that responded similarly over the thermal gradient were identified using SoftClustering following reference 89. A matrix of *n* genes × 9 treatments (4 temperatures at nighttime and 5 temperatures at daytime) was used as input data. Data for each gene were standardized to zero mean and unit variance. The optimal value of the parameter *m* in the Mfuzz algorithm was estimated through randomization following reference 90. The number of clusters was chosen to maximize the functional enrichment of gene clusters (COGs) and the ClusterJudge method (91). The standardized data were clustered by a generalized version of the Fuzzy c-means algorithm. Finally, statistically significant differences in cellular transcript concentration among temperature regimes were determined by the Kruskall-Wallis test using R.

Data availability. Raw reads have been submitted to ENA under project no. PRJEB54738 (accession no. ERS12467859 to ERS12467904).

SUPPLEMENTAL MATERIAL

Supplemental material is available online only.

FIG S1, PDF file, 0.3 MB.
FIG S2, PDF file, 0.3 MB.
FIG S3, PDF file, 0.4 MB.
TABLE S1, XLSX file, 0.01 MB.
TABLE S2, XLSX file, 0.5 MB.
TABLE S3, XLSX file, 1.1 MB.
TABLE S4, XLSX file, 1.1 MB.
TABLE S5, XLSX file, 0.2 MB.
TABLE S6, XLSX file, 0.01 MB.
TABLE S7, XLSX file, 0.2 MB.

ACKNOWLEDGMENTS

We are grateful to the Spanish Ministry of Economy and Competitiveness (MINECO) for supporting L.A.-S.'s Ramón y Cajal research contract (RYC-2012-11404), A.S.P.'s FPI Ph.D. fellowship (BES2015076149), and the project TECCAM (CTM2014-58564-R) and the Spanish Ministry of Science and Innovation for supporting the project CYADES (RTI2018-100690-B-I00). S.R.-E. and J.M.G. were supported by project PID2019-110011RB-C32 (Spanish Ministry of Science and Innovation, Spanish State Research Agency). The Department of Economic Development, Sustainability and Environment of the Basque Government is acknowledged for funding the project BIOMATRIX. L.G. acknowledges funding from the Agence Nationale de la Recherche project CINNAMON (ANR-17-CE2-0014-01).

REFERENCES

1. Partensky F, Hess WR, Vaulot D. 1999. *Prochlorococcus*, a marine photosynthetic prokaryote of global significance. Microbiol Mol Biol Rev 63:106–127. https://doi.org/10.1128/MMBR.63.1.106-127.1999.
2. Li W. 1994. Primary production of prochlorophytes, cyanobacteria, and eucaryotic ultraphytoplankton: measurements from flow cytometric sorting. Limnol Oceanogr 39:169–175. https://doi.org/10.4319/lo.1994.39.1.0169.

3. Johnson ZI, Zinser ER, Coe A, McNulty NP, Woodward EMS, Chisholm SW. 2006. Niche partitioning among *Prochlorococcus* ecotypes along ocean-scale environmental gradients. Science 311:1737–1740. https://doi.org/10.1126/science.1118052.
4. Flombaum P, Gallegos JL, Gordillo RA, Rincón J, Zabala LL, Jiao N, Karl DM, Li WKW, Lomas MW, Veneziano D, Vera CS, Vrugt JA, Martiny AC. 2013. Present and future global distributions of the marine cyanobacteria *Prochlorococcus* and *Synechococcus*. Proc Natl Acad Sci U S A 110:9824–9829. https://doi.org/10.1073/pnas.1307701110.
5. Follett CL, Dutkiewicz S, Ribalet F, Zakem E, Caron D, Armbrust EV, Follows MJ. 2022. Trophic interactions with heterotrophic bacteria limit the range of *Prochlorococcus*. Proc Natl Acad Sci U S A 119:e2110993118. https://doi.org/10.1073/pnas.2110993118.
6. Zinser ER, Johnson ZI, Coe A, Karaca E, Veneziano D, Chisholm SW. 2007. Influence of light and temperature on *Prochlorococcus* ecotype distributions in the Atlantic Ocean. Limnol Oceanogr 52:2205–2220. https://doi.org/10.4319/lo.2007.52.5.2205.
7. Moore LR, Goericke R, Chisholm SW. 1995. Comparative physiology of *Synechococcus* and *Prochlorococcus*: influence of light and temperature on growth, pigments, fluorescence and absorptive properties. Mar Ecol Prog Ser 116:259–276. https://doi.org/10.3354/meps116259.
8. Scanlan DJ, Ostrowski M, Mazard S, Dufresne A, Garczarek L, Hess WR, Post AF, Hagemann M, Paulsen I, Partensky F. 2009. Ecological genomics of marine picocyanobacteria. Microbiol Mol Biol Rev 73:249–299. https://doi.org/10.1128/MMBR.00035-08.
9. Partensky F, Garczarek L. 2010. *Prochlorococcus*: advantages and limits of minimalism. Annu Rev Mar Sci 2:305–331. https://doi.org/10.1146/annurev-marine-120308-081034.
10. Mary I, Vaulot D. 2003. Two-component systems in Prochlorococcus MED4: genomic analysis and differential expression under stress. FEMS Microbiol Lett 226:135–144. https://doi.org/10.1016/S0378-1097(03)00587-1.
11. Kingsolver JG. 2009. The well-temperatured biologist. Am Nat 174:755–768. https://doi.org/10.1086/648310.
12. Mackey KRM, Paytan A, Caldeira K, Grossman AR, Moran D, Mcilvin M, Saito MA. 2013. Effect of temperature on photosynthesis and growth in marine *Synechococcus* spp. Plant Physiol 163:815–829. https://doi.org/10.1104/pp.113.221937.
13. Pittera J, Humily F, Thorel M, Grulois D, Garczarek L, Six C. 2014. Connecting thermal physiology and latitudinal niche partitioning in marine *Synechococcus*. ISME J 8:1221–1236. https://doi.org/10.1038/ismej.2013.228.
14. Pittera J, Partensky F, Six C. 2017. Adaptive thermostability of light-harvesting complexes in marine picocyanobacteria. ISME J 11:112–124. https://doi.org/10.1038/ismej.2016.102.
15. Bailey S, Grossman A. 2008. Photoprotection in cyanobacteria: regulation of light harvesting. Photochem Photobiol 84:1410–1420. https://doi.org/10.1111/j.1751-1097.2008.00453.x.
16. Yamamoto Y. 2016. Quality control of photosystem II: the mechanisms for avoidance and tolerance of light and heat stresses are closely linked to membrane fluidity of the thylakoids. Front Plant Sci 7:1136. https://doi.org/10.3389/fpls.2016.01136.
17. Murata N, Takahashi S, Nishiyama Y, Allakhverdiev SI. 2007. Photoinhibition of photosystem II under environmental stress. Biochim Biophys Acta Bioenerg 1767:414–421. https://doi.org/10.1016/j.bbabio.2006.11.019.
18. Pospíšil P, Tyystjärvi E. 1999. Molecular mechanism of high-temperature-induced inhibition of acceptor side of photosystem II. Photosynth Res 62:55–66. https://doi.org/10.1023/A:1006369009170.
19. Mathur S, Agrawal D, Jajoo A. 2014. Photosynthesis: response to high temperature stress. J Photochem Photobiol B Biol 137:116–126. https://doi.org/10.1016/j.jphotobiol.2014.01.010.
20. Varkey D, Mazard S, Ostrowski M, Tetu SG, Haynes P, Paulsen IT. 2016. Effects of low temperature on tropical and temperate isolates of marine *Synechococcus*. ISME J 10:1252–1263. https://doi.org/10.1038/ismej.2015.179.
21. Toseland A, Daines SJ, Clark JR, Kirkham A, Strauss J, Uhlig C, Lenton TM, Valentin K, Pearson GA, Moulton V, Mock T. 2013. The impact of temperature on marine phytoplankton resource allocation and metabolism. Nat Clim Chang 3:979–984. https://doi.org/10.1038/nclimate1989.
22. Guyet U, Nguyen NA, Doré H, Haguait J, Pittera J, Conan M, Ratin M, Corre E, Le Corguillé G, Brillet-Guéguen L, Hoebeke M, Six C, Steglich C, Siegel A, Eveillard D, Partensky F, Garczarek L. 2020. Synergic effects of temperature and irradiance on the physiology of the marine *Synechococcus* strain WH7803. Front Microbiol 11:1707. https://doi.org/10.3389/fmicb.2020.01707.
23. Roth Rosenberg D, Haber M, Goldford J, Lalzar M, Aharonovich D, Al-Ashhab A, Lehahn Y, Segrè D, Steindler L, Sher D. 2021. Particle-associated and free-living bacterial communities in an oligotrophic sea are affected by different environmental factors. Environ Microbiol 23:4295–4308. https://doi.org/10.1111/1462-2920.15611.
24. Mikami K, Murata N. 2003. Membrane fluidity and the perception of environmental signals in cyanobacteria and plants. Prog Lipid Res 42:527–543. https://doi.org/10.1016/s0163-7827(03)00036-5.
25. Los DA, Murata N. 1999. Responses to cold shock in cyanobacteria. J Mol Microbiol Biotechnol 1:221–230.
26. Liang Y, Koester JA, Liefer JD, Irwin AJ, Finkel ZV. 2019. Molecular mechanisms of temperature acclimation and adaptation in marine diatoms. ISME J 13:2415–2425. https://doi.org/10.1038/s41396-019-0441-9.
27. Murayama Y, Kori H, Oshima C, Kondo T, Iwasaki H, Ito H. 2017. Low temperature nullifies the circadian clock in cyanobacteria through Hopf bifurcation. Proc Natl Acad Sci U S A 114:5641–5646. https://doi.org/10.1073/pnas.1620378114.
28. Rajaram H, Chaurasia AK, Apte SK. 2014. Cyanobacterial heat-shock response: role and regulation of molecular chaperones. Microbiology 160:647–658. https://doi.org/10.1099/mic.0.073478-0.
29. Farrant GK, Doré H, Cornejo-Castillo FM, Partensky F, Ratin M, Ostrowski M, Pitt FD, Wincker P, Scanlan DJ, Iudicone D, Acinas SG, Garczarek L. 2016. Delineating ecologically significant taxonomic units from global patterns of marine picocyanobacteria. Proc Natl Acad Sci U S A 113:E3365–E3374. https://doi.org/10.1073/pnas.1524865113.
30. Huang S, Wilhelm SW, Harvey HR, Taylor K, Jiao N, Chen F. 2012. Novel lineages of *Prochlorococcus* and *Synechococcus* in the global oceans. ISME J 6:285–297. https://doi.org/10.1038/ismej.2011.106.
31. Kettler GC, Martiny AC, Huang K, Zucker J, Coleman ML, Rodrigue S, Chen F, Lapidus A, Ferriera S, Johnson J, Steglich C, Church GM, Richardson P, Chisholm SW. 2007. Patterns and implications of gene gain and loss in the evolution of *Prochlorococcus*. PLoS Genet 3:2515–2528. https://doi.org/10.1371/journal.pgen.0030231.
32. Moran MA, Satinsky B, Gifford SM, Luo H, Rivers A, Chan LK, Meng J, Durham BP, Shen C, Varaljay VA, Smith CB, Yager PL, Hopkinson BM. 2013. Sizing up metatranscriptomics. ISME J 7:237–243. https://doi.org/10.1038/ismej.2012.94.
33. Gifford SM, Becker JW, Sosa OA, Repeta DJ, DeLong EF. 2016. Quantitative transcriptomics reveals the growth- and nutrient-dependent response of a streamlined marine methylotroph to methanol and naturally occurring dissolved organic matter. mBio 7:e01279-16. https://doi.org/10.1128/mBio.01279-16.
34. Zinser ER, Lindell D, Johnson ZI, Futschik ME, Steglich C, Coleman ML, Wright MA, Rector T, Steen R, McNulty N, Thompson LR, Chisholm SW. 2009. Choreography of the transcriptome, photophysiology, and cell cycle of a minimal photoautotroph, *Prochlorococcus*. PLoS One 4:e5135. https://doi.org/10.1371/journal.pone.0005135.
35. Bae W, Xia B, Inouye M, Severinov K. 2000. *Escherichia coli* CspA-family RNA chaperones are transcription antiterminators. Proc Natl Acad Sci U S A 97:7784–7789. https://doi.org/10.1073/pnas.97.14.7784.
36. Watanabe S, Sato M, Nimura-Matsune K, Chibazakura T, Yoshikawa H. 2007. Protection of psbAII transcript from ribonuclease degradation in vitro by DnaK2 and DnaJ2 chaperones of the cyanobacterium *Synechococcus elongatus* PCC 7942. Biosci Biotechnol Biochem 71:279–282. https://doi.org/10.1271/bbb.60647.
37. Bagby SC, Chisholm SW. 2015. Response of Prochlorococcus to varying CO_2:O_2 ratios. ISME J 9:2232–2245. https://doi.org/10.1038/ismej.2015.36.
38. Mella-Flores D, Six C, Ratin M, Partensky F, Boutte C, Le Corguillé G, Marie D, Blot N, Gourvil P, Kolowrat C, Garczarek L. 2012. *Prochlorococcus* and *Synechococcus* have evolved different adaptive mechanisms to cope with light and UV stress. Front Microbiol 3:285. https://doi.org/10.3389/fmicb.2012.00285.
39. Salazar G, Paoli L, Alberti A, Huerta-Cepas J, Ruscheweyh HJ, Cuenca M, Field CM, Coelho LP, Cruaud C, Engelen S, Gregory AC, Labadie K, Marec C, Pelletier E, Royo-Llonch M, Roux S, Sánchez P, Uehara H, Zayed AA, Zeller G, Carmichael M, Dimier C, Ferland J, Kandels S, Picheral M, Pisarev S, Poulain J, Acinas SG, Babin M, Bork P, Boss E, Bowler C, Cochrane G, de Vargas C, Follows M, Gorsky G, Grimsley N, Guidi L, Hingamp P, Iudicone D, Jaillon O, Kandels-Lewis S, Karp-Boss L, Karsenti E, Not F, Ogata H, Pesant S, Poulton N, Raes J, Sardet C, Tara Oceans Coordinators, et al. 2019. Gene expression changes and community turnover differentially shape the global ocean metatranscriptome. Cell 179:1068–1083.e21. https://doi.org/10.1016/j.cell.2019.10.014.
40. Six C, Ratin M, Marie D, Corre E. 2021. Marine *Synechococcus* picocyanobacteria: light utilization across latitudes. Proc Natl Acad Sci U S A 118:e2111300118. https://doi.org/10.1073/pnas.2111300118.
41. Ferrieux M, Dufour L, Doré H, Ratin M, Guéneuguès A, Chasselin L, Marie D, Rigaut-Jalabert F, Le Gall F, Sciandra T, Monier G, Hoebeke M, Corre E,

Xia X, Liu H, Scanlan DJ, Partensky F, Garczarek L. 2022. Comparative thermophysiology of marine *Synechococcus* CRD1 strains isolated from different thermal niches in iron-depleted areas. Front Microbiol 13:e3893413. https://doi.org/10.3389/fmicb.2022.893413.
42. Pittera J, Jouhet J, Breton S, Garczarek L, Partensky F, Maréchal É, Nguyen NA, Doré H, Ratin M, Pitt FD, Scanlan DJ, Six C. 2018. Thermoacclimation and genome adaptation of the membrane lipidome in marine *Synechococcus*. Environ Microbiol 20:612–631. https://doi.org/10.1111/1462-2920.13985.
43. Ma L, Calfee BC, Morris JJ, Johnson ZI, Zinser ER. 2018. Degradation of hydrogen peroxide at the ocean's surface: the influence of the microbial community on the realized thermal niche of *Prochlorococcus*. ISME J 12:473–484. https://doi.org/10.1038/ismej.2017.182.
44. Zinser ER. 2018. Cross-protection from hydrogen peroxide by helper microbes: the impacts on the cyanobacterium Prochlorococcus and other beneficiaries in marine communities. Environ Microbiol Rep 10:399–411. https://doi.org/10.1111/1758-2229.12625.
45. Lima-Melo Y, Alencar VTCB, Lobo AKM, Sousa RHV, Tikkanen M, Aro EM, Silveira JAG, Gollan PJ. 2019. Photoinhibition of photosystem I provides oxidative protection during imbalanced photosynthetic electron transport in *Arabidopsis thaliana*. Front Plant Sci 10:916. https://doi.org/10.3389/fpls.2019.00916.
46. Muramatsu M, Hihara Y. 2003. Transcriptional regulation of genes encoding subunits of photosystem I during acclimation to high-light conditions in *Synechocystis* sp. PCC 6803. Planta 216:446–453. https://doi.org/10.1007/s00425-002-0859-5.
47. Thompson Huang K, Saito MA, Chisholm SW. 2011. Transcriptome response of high- and low-light-adapted *Prochlorococcus* strains to changing iron availability. ISME J 5:1580–1594. https://doi.org/10.1038/ismej.2011.49.
48. Thompson LR, Zeng Q, Chisholm SW. 2016. Gene expression patterns during light and dark infection of *Prochlorococcus* by cyanophage. PLoS One 11:1–20. https://doi.org/10.1371/journal.pone.0165375.
49. Steglich C, Futschik M, Rector T, Steen R, Chisholm SW. 2006. Genome-wide analysis of light sensing in *Prochlorococcus*. J Bacteriol 188:7796–7806. https://doi.org/10.1128/JB.01097-06.
50. Mattoo AK, Giardi MT, Raskind A, Edelman M. 1999. Dynamic metabolism of photosystem II reaction center proteins and pigments. Physiol Plant 107:454–461. https://doi.org/10.1034/j.1399-3054.1999.100412.x.
51. Garczarek L, Partensky F, Irlbacher H, Holtzendorff J, Babin M, Mary I, Thomas JC, Hess WR. 2001. Differential expression of antenna and core genes in Prochlorococcus PCC 9511 (Oxyphotobacteria) grown under a modulated light-dark cycle. Environ Microbiol 3:168–175. https://doi.org/10.1046/j.1462-2920.2001.00173.x.
52. Holtzendorff J, Partensky F, Mella D, Lennon JF, Hess WR, Garczarek L. 2008. Genome streamlining results in loss of robustness of the circadian clock in the marine cyanobacterium *Prochlorococcus marinus* PCC 9511. J Biol Rhythms 23:187–199. https://doi.org/10.1177/0748730408316040.
53. Sonoike K. 2011. Photoinhibition of photosystem I. Physiol Plant 142:56–64. https://doi.org/10.1111/j.1399-3054.2010.01437.x.
54. Bailey S, Melis A, Mackey KRM, Cardol P, Finazzi G, van Dijken G, Berg GM, Arrigo K, Shrager J, Grossman A. 2008. Alternative photosynthetic electron flow to oxygen in marine *Synechococcus*. Biochim Biophys Acta Bioenerg 1777:269–276. https://doi.org/10.1016/j.bbabio.2008.01.002.
55. Biller SJ, Coe A, Roggensack SE, Chisholm W. 2018. Heterotroph interactions alter Prochlorococcus transcriptome. mSystems 3:e00040-18. https://doi.org/10.1128/mSystems.00040-18.
56. Imamura S, Asayama M. 2009. Sigma factors for cyanobacterial transcription. Gene Regul Syst Biol 3:65–87. https://doi.org/10.4137/grsb.s2090.
57. Summerfield TC, Sherman LA. 2007. Role of sigma factors in controlling global gene expression in light/dark transitions in the cyanobacterium *Synechocystis* sp. strain PCC 6803. J Bacteriol 189:7829–7840. https://doi.org/10.1128/JB.01036-07.
58. van Waasbergen LG, Dolganov N, Grossman AR. 2002. nblS, a gene involved in controlling photosynthesis-related gene expression during high light and nutrient stress in *Synechococcus elongatus* PCC 7942. J Bacteriol 184:2481–2490. https://doi.org/10.1128/JB.184.9.2481-2490.2002.
59. Espinosa J, Boyd JS, Cantos R, Salinas P, Golden SS, Contreras A. 2015. Cross-talk and regulatory interactions between the essential response regulator RpaB and cyanobacterial circadian clock output. Proc Natl Acad Sci U S A 112:2198–2203. https://doi.org/10.1073/pnas.1424632112.
60. Takai N, Nakajima M, Oyama T, Kito R, Sugita C, Sugita M, Kondo T, Iwasaki H. 2006. A KaiC-associating SasA-RpaA two-component regulatory system as a major circadian timing mediator in cyanobacteria. Proc Natl Acad Sci U S A 103:12109–12114. https://doi.org/10.1073/pnas.0602955103.
61. Steglich C, Lindell D, Futschik M, Rector T, Steen R, Chisholm SW. 2010. Short RNA half-lives in the slow-growing marine cyanobacterium *Prochlorococcus*. Genome Biol 11:R54. https://doi.org/10.1186/gb-2010-11-5-r54.
62. Jacquet S, Partensky F, Marie D, Casotti R, Vaulot D. 2001. Cell cycle regulation by light in *Prochlorococcus* strains. Appl Environ Microbiol 67:782–790. https://doi.org/10.1128/AEM.67.2.782-790.2001.
63. Shalapyonok A, Olson RJ, Shalapyonok LS. 1998. Ultradian growth in *Prochlorococcus* spp. Appl Environ Microbiol 64:1066–1069. https://doi.org/10.1128/AEM.64.3.1066-1069.1998.
64. Palacio AS, Cabello AM, García FC, Labban A, Morán XAG, Garczarek L, Alonso-Sáez L, López-Urrutia Á. 2020. Changes in population age-structure obscure the temperature-size rule in marine cyanobacteria. Front Microbiol 11:2059. https://doi.org/10.3389/fmicb.2020.02059.
65. Ting CS, Hambleton E, McKenna J. 2008. Photosynthetic response to environmental stress in Prochlorococcus, p 1585–1588. *In* Allen JF, Gantt E, Golbeck JH, Osmond B (ed), Photosynthesis. Energy from the sun. Springer, Dordrecht, The Netherlands.
66. Moreno AR, Martiny AC. 2018. Ecological stoichiometry of ocean plankton. Annu Rev Mar Sci 10:43–69. https://doi.org/10.1146/annurev-marine-121916-063126.
67. Swain PS, Elowitz MB, Siggia ED. 2002. Intrinsic and extrinsic contributions to stochasticity in gene expression. Proc Natl Acad Sci U S A 99:12795–12800. https://doi.org/10.1073/pnas.162041399.
68. Thattai M, Van Oudenaarden A. 2001. Intrinsic noise in gene regulatory networks. Proc Natl Acad Sci U S A 98:8614–8619. https://doi.org/10.1073/pnas.151588598.
69. Axmann IM, Dühring U, Seeliger L, Arnold A, Vanselow JT, Kramer A, Wilde A. 2009. Biochemical evidence for a timing mechanism in Prochlorococcus. J Bacteriol 191:5342–5347. https://doi.org/10.1128/JB.00419-09.
70. Rippka R, Coursin T, Hess W, Lichtle C, Scanlan DJ, Palinska KA, Iteman I, Partensky F, Houmard J, Herdman M. 2000. *Prochlorococcus marinus* Chisholm et al. 1992 subsp. pastoris subsp. nov. strain PCC 9511, the first axenic chlorophyll a2/b2-containing cyanobacterium (Oxyphotobacteria). Int J Syst Evol Microbiol 50:1833–1847. https://doi.org/10.1099/00207713-50-5-1833.
71. Calvo-Díaz A, Morán XAG. 2006. Seasonal dynamics of picoplankton in shelf waters of the southern Bay of Biscay. Aquat Microb Ecol 42:159–174. https://doi.org/10.3354/ame042159.
72. Andrews S. 2020. FastQC: a quality control tool for high throughput sequence data. http://www.bioinformatics.babraham.ac.uk/projects/fastqc.
73. Bolger AM, Lohse M, Usadel B. 2014. Trimmomatic: a flexible trimmer for Illumina sequence data. Bioinformatics 30:2114–2120. https://doi.org/10.1093/bioinformatics/btu170.
74. Kopylova E, Noé L, Touzet H. 2012. SortMeRNA: fast and accurate filtering of ribosomal RNAs in metatranscriptomic data. Bioinformatics 28:3211–3217. https://doi.org/10.1093/bioinformatics/bts611.
75. Langmead B, Salzberg SL. 2012. Fast gapped-read alignment with Bowtie 2. Nat Methods 9:357–359. https://doi.org/10.1038/nmeth.1923.
76. Anders S, Pyl PT, Huber W. 2015. HTSeq—a Python framework to work with high-throughput sequencing data. Bioinformatics 31:166–169. https://doi.org/10.1093/bioinformatics/btu638.
77. Gifford S, Satinsky B, Moran MA. 2014. Quantitative microbial metatranscriptomics. *In* Paulsen I, Holmes A (eds), Environmental microbiology. Methods in molecular biology vol 1096. Humana Press, Totowa, NJ. https://doi.org/10.1007/978-1-62703-712-9_17.
78. Kempe H, Schwabe A, Crémazy F, Verschure PJ, Bruggeman FJ. 2015. The volumes and transcript counts of single cells reveal concentration homeostasis and capture biological noise. Mol Biol Cell 26:797–804. https://doi.org/10.1091/mbc.E14-08-1296.
79. Zhurinsky J, Leonhard K, Watt S, Marguerat S, Bähler J, Nurse P. 2010. A coordinated global control over cellular transcription. Curr Biol 20:2010–2015. https://doi.org/10.1016/j.cub.2010.10.002.
80. Love MI, Huber W, Anders S. 2014. Moderated estimation of fold change and dispersion for RNA-seq data with DESeq2. Genome Biol 15:550. https://doi.org/10.1186/s13059-014-0550-8.
81. Chen S, Zhou Y, Chen Y, Gu J. 2018. Fastp: An ultra-fast all-in-one FASTQ preprocessor. Bioinformatics 34:i884–i890. https://doi.org/10.1093/bioinformatics/bty560.
82. Deng Z-L, Münch PC, Mreches R, McHardy AC. 2022. Rapid and accurate identification of ribosomal RNA sequences via deep learning. Nucleic Acids Res 50:e60. https://doi.org/10.1093/nar/gkac112.
83. Klemetsen T, Raknes IA, Fu J, Agafonov A, Balasundaram SV, Tartari G, Robertsen E, Willassen NP. 2018. The MAR databases: development and implementation of databases specific for marine metagenomics. Nucleic Acids Res 46:D693–D699. https://doi.org/10.1093/nar/gkx1036.

84. Pruitt KD, Tatusova T, Maglott DR. 2007. NCBI Reference Sequence (RefSeq): a curated non-redundant sequence database of genomes, transcripts and proteins. Nucleic Acids Res 35(Database issue):D61–D65. https://doi.org/10.1093/nar/gkl842.
85. Li H, Durbin R. 2009. Fast and accurate short read alignment with Burrows-Wheeler transform. Bioinformatics 25:1754–1760. https://doi.org/10.1093/bioinformatics/btp324.
86. Putri GH, Anders S, Pyl PT, Pimanda JE, Zanini F. 2022. Analysing high-throughput sequencing data in Python with HTSeq 2.0. Bioinformatics 38:2943–2945. https://doi.org/10.1093/bioinformatics/btac166.
87. Cock PJA, Antao T, Chang JT, Chapman BA, Cox CJ, Dalke A, Friedberg I, Hamelryck T, Kauff F, Wilczynski B, De Hoon MJL. 2009. Biopython: freely available Python tools for computational molecular biology and bioinformatics. Bioinformatics 25:1422–1423. https://doi.org/10.1093/bioinformatics/btp163.
88. Robaina-Estévez S. 2023. Robaina/Prochlorococcus. GitHub https://github.com/Robaina/prochlorococcus. Accessed 22 July 2022.
89. Kumar L, Futschik ME. 2007. Mfuzz: A software package for soft clustering of microarray data. Bioinformation 2:5–7. https://doi.org/10.6026/97320630002005.
90. Schwämmle V, Jensen ON. 2010. A simple and fast method to determine the parameters for fuzzy c-means cluster analysis. Bioinformatics 26:2841–2848. https://doi.org/10.1093/bioinformatics/btq534.
91. Pasculescu A. 2022. ClusterJudge. https://bioconductor.org/packages/release/bioc/html/ClusterJudge.html.